Nonisothermal Crystallization Kinetics and Morphology of Self-Seeded Syndiotactic 1,2-Polybutadiene

Jiali Cai,[1,2] Tao Li,[1] Ying Han,[1] Yuanqi Zhuang,[1] Xuequan Zhang[3]

[1]*Key Laboratory for Ultrafine Materials of Ministry of Education, School of Materials Science and Engineering, East China University of Science and Technology, Shanghai 200237, People's Republic of China*
[2]*Department of Polymer Materials and Engineering, College of Chemistry and Chemical Engineering, Nanjing University, Nanjing 210093, People's Republic of China*
[3]*State Key Laboratory of Polymer Physics and Chemistry, Changchun Institute of Applied Chemistry, Chinese Academy of Sciences, Changchun 130022, People's Republic of China*

Received 10 May 2005; accepted 1 September 2005
DOI 10.1002/app.23147
Published online in Wiley InterScience (www.interscience.wiley.com).

ABSTRACT: Subsequent melting behavior after isothermal crystallization at different temperatures from the isotropic melt and nonisothermal crystallization kinetics and morphology of partially melting sPB were carried out by differential scanning calorimetry (DSC), polarized light microscopy (POM), respectively. Triple melting-endothermic peaks were observed for the polymer first isothermally crystallized at temperatures ranging from 141 to 149°C, respectively, and then followed by cooling at 10°C/min to 70°C. Comparing with the nonisothermal crystallization from the isotropic melt, the nonisothermal crystallization for the partially melting sPB characterized the increased onset crystallization temperature, and the sizes of spherulites became smaller and more uniform. The Tobin, Avrami, Ozawa, and the combination of Avrami and Ozawa equations were applied to describe the kinetics of the nonisothermal process. Both of the Tobin and the Avrami crystallization rate parameters (K_T and K_A, respectively) were found to increase with increase in the cooling rate. The parameter $F(T)$ for the combination of Avrami and Ozawa equations increases with increasing relative crystallinity. The Ziabicki's kinetic crytallizability index G_Z for the partially melting sPB was found to be 3.14. The effective energy barrier ΔE describing the nonisothermal crystallization of partially melting sPB was evaluated by the differential isoconversional method of Friedman and was found to increase with an increase in the relative crystallinity. At the same time, Hoffman-Lauritzen parameters (U and K_g) are evaluated and analyzed from the nonisothermal crystallization data by the combination of isoconversional approach and Hoffman-Lauritzen theory. The K_g value obtained from DSC technique was found to be in good agreement with that obtained from POM technique. © 2006 Wiley Periodicals, Inc. J Appl Polym Sci 100: 1479–1491, 2006

Key words: syndiotactic 1,2-polybutadiene; nonisothermal crystallization; kinetics; activation energy; differential scanning calorimetry

INTRODUCTION

Commonly, crystallization process of semicrystalline polymers involves induction period, nucleation, and crystal growth. Any variation, especially in the step of nucleation or crystal growth, would necessarily change the end-morphology, which is closely correlated with properties of these materials.[1] Therefore, studies on crystallization mechanisms of polymers will provide more insights into controlling and improving properties of polymer products. Many studies have indicated that addition of nucleation agents or additives improved the nucleation density and crystallization rate, and increased the number of spherulites in unit area.[2–5] Bank et al. first proposed a method named as "self-nucleation" to explore the relationship between molten temperature and crystallization behavior of polyethylene (PE).[6] As the crystallized PE was partially molten at temperature below the melting point, followed by crystallizing in the presence of the unmolten crystallized samples, it was found that the crystallization rate of PE sample improved greatly. Later on, many experimental[7–15] and theoretical[16–18] studies in the self-nucleation field have been carried out. These results indicated that the self-nucleation procedure not only speeds up the crystallization rate, similar to the cases of addition of some nucleation agents,[2–5] but also make the Avrami exponent n_A, obtained from the partially melting sample, different from that obtained from the isotropic melt.

Syndiotactic 1,2-polybutadiene (sPB) is also a typical semicrystalline polymer, which was first synthe-

Correspondence to: J. Cai (jlcai@ecust.edu.cn).
Contract grant sponsor: National Natural Science Foundation of China; contract grant number: 20274046.
Contract grant sponsor: The State Key Laboratory of Polymer Physics and Chemistry.
Contract grant sponsor: Specialized Research Fund for the Doctoral Program of Higher Education of China; contract grant number: 20030284003.

sized by Natta and Corradini,[19] and are widely used as packaging films, rubber goods, adhesive, oil point, photosensitive resin, plastics materials, etc.[19,20] Consequently the studies of crystallization mechanisms on sPB are not only of theoretical significance, but also of value in practical applications. Up to now, crystallization studies on sPB are still exiguous. A few studies[19,21–26] on crystal structure, crystalline morphology, and crystallization kinetics have been carried out.

The present contribution is aimed at studying the nonisothermal crystallization kinetics of partially melting sPB in full. The experimental data, for different cooling rates ranging from 2.5 to 60°C/min, were obtained from the differential scanning calorimetry (DSC) technique and were thoroughly analyzed based on Tobin, Avrami, Ozawa; the combination of Avrami and Ozawa; and Ziabicki macrokinetic models. The effective energy barrier describing the nonisothermal crystallization process of partially sPB was estimated based on the differential isoconversional method of Friedman, and Hoffman-Lauritzen parameters (U and K_g) are evaluated and analyzed by the combination of isoconversional approach and Hoffman-Lauritzen theory. At the same time, polarized light microscopy (POM) was utilized to investigate the morphology crystallized from the partially melting sPB.

EXPERIMENTAL

Materials

The catalyst system for the synthesis of syndiotactic 1,2-polybutadiene (sPB) was a new iron one, which was composed of Iron (III) acetylacetonate(Fe(acac)$_3$), Triisobutylaluminum, and Diethyl phosphite(DEP). The detailed procedure for synthesizing the sample has been presented elsewhere.[27] The molecular weight of the sPB sample is $M_w = 1.38 \times 10^6$, and $M_w/M_n = 2.4$, measured by high temperature GPC after dissolving the sample in trichlorobenzene (TCB) at 150°C. The degree of syndiotacticity of the sPB was determined to be 89% by ^{13}C NMR, after it was dissolved in d4-*O*-dichlorobenzene at 135°C.

Sample preparation and experimental details

The sheets of the sPB sample were prepared by pressing the powder under pressure of 5 MPa at 200°C between polytetrafluoroethylene films and quickly cooling down to ice temperature. The obtained sheets were used for DSC experiments.

A Perkin–Elmer Diamond DSC calibrated with indium and zinc standards was used to monitor the nonisothermal crystallization kinetics of the partially melting sPB samples. For minimizing thermal lag between the polymer sample and the DSC furnace, the sheets were cut into disk-shaped pieces, and the sample weights were 8–9 mg.

For the subsequently melting experiments after isothermal crystallization, the sPB sample sheets were first heated at 100°C/min from 50 to 200°C and kept at 200°C for 2 min to eliminate residual crystals. The samples were then cooled from 200°C/min to the preset temperatures (141, 143, 145, 147, and 149°C) and isothermally crystallized at these temperatures for 60 min, respectively. The crystallized materials were then cooled to 70°C at 10°C/min, followed by heating at 10°C/min from 70 to 200°C.

For the nonisothermal crystallization experiments, the sPB sample was first isothermally crystallized at 145°C for 60 min, according to the procedures described earlier for the isothermal crystallization operations, and then directly heated at 10°C/min to 171°C. On reaching 171°C, the sample was cooled at different rates (2.5, 5, 10, 20, 30, 40, 60°C/min) to 70°C. The relative crystallinity at a definite time and temperature was calculated by the supplied software of this instrument for further analysis of various macro-kinetic models.

The crystalline morphology of the sPB sample was observed by a polarized optical microscope (Leika) equipped with an automatic thermal control hot-stage with controlling temperature precision of ±0.1°C. The sPB samples sandwiched between microscope cover glasses were first heated to 200°C, and then cooled at 100°C/min to 145°C to be held for 60 min, after that they were heated to 171 and 200°C, respectively, followed at last by cooling at 10°C/min.

Measurements of the spherulite growth rates were carried out according to the following procedure: the sPB samples sandwiched between microcope cover glasses were first heated to 200°C, and then cooled at 100°C/min to the designated temperatures (142, 144, 146, 148, and 150°C).

RESULTS AND DISCUSSION

Nonisothermal crystallization and morphology of partially melting sPB

The melting thermographs for sPB isothermally crystallized at 141, 143, 145, 147, and 149°C for 60 min, respectively, are shown in the inset figure of Figure 1. The samples were first crystallized at these temperatures and then cooled to 70°C, followed by heating at a rate of 10°C/min from 70 to 200°C. Clearly, triple-melting endothermic peaks appear for all investigated temperatures. The high, middle, and low melting endothermic peaks are marked as 1, 2, and 3, respectively. Peak temperature of 3 is lower than the crystallized temperature and derived from recrystallization during cooling and heating scans between 70 and 145°C. peak 2 was found to correspond to the melting

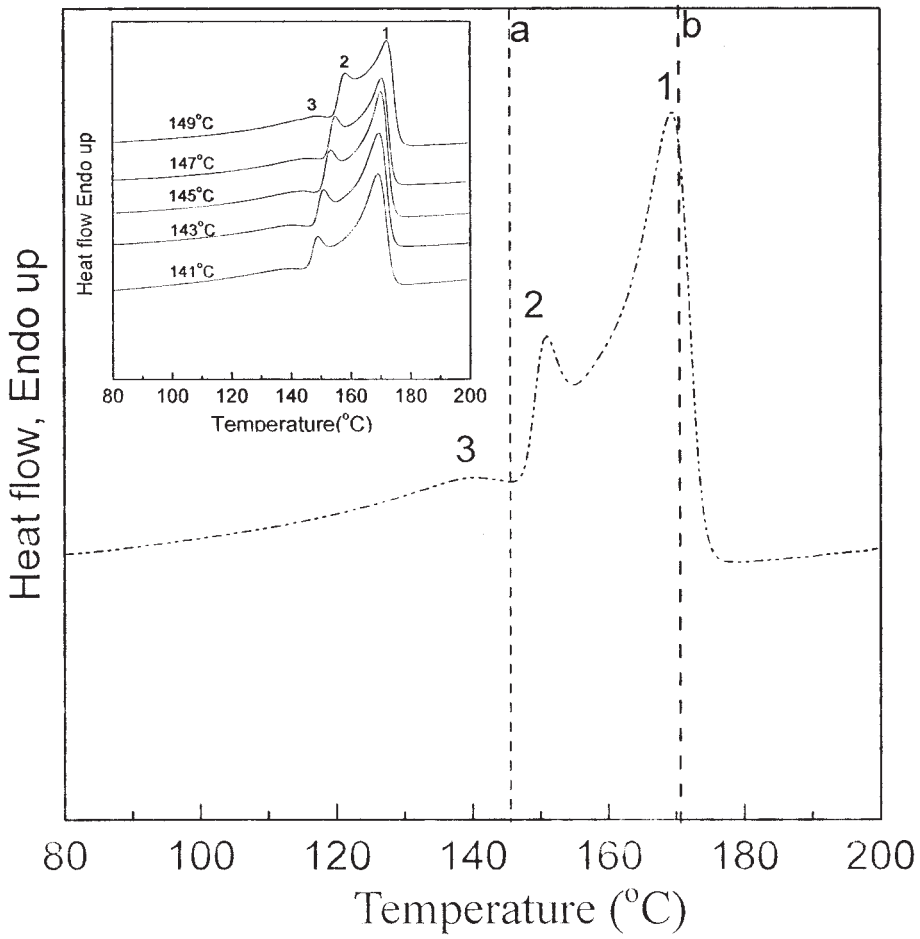

Figure 1 Melting endothermic curve of syndiotactic 1,2-polybutadiene first crystallized at 145°C for 1 h and cooled at 100°C/min to 70°C, followed by heating at 10°C/min from 70 to 200°C. a and b indicate the positions of 145 and 171°C. Numbers 1, 2, and 3 designate the melting peaks, according to the temperature sequence from high to low. The inserted figure indicates the melting curves of syndiotactic 1,2-polybutadiene crystallized at 141, 143, 145, 147, and 149°C.

of the primary crystallites formed at a definite crystallization temperature and peak 3 corresponds to the melting of recrystallized crystallites, which were formed during a heating scan.[1] Figure 1 (inset) shows that peaks 2 and 3 increase with increasing crystallized temperature, while increases in peak 1 are less than the other two peaks, ranging between 169.4 and 171.5°C. At 145°C, peak temperature of 1 is 170.3°C; therefore, we selected 171°C (marked as b in Fig. 1 and just higher than the peak temperature of 1) as the temperature for melting most of the crystalline materials crystallized at 145°C. After the samples were melt-crystallized at 145°C for 60 min, they were heated at 10°C/min from 145 to 171°C, and on reaching 171°C, they were cooled to 70°C at different cooling rates (2.5, 5, 10, 20, 30, 40, and 60°C/min), respectively.

For the purpose of comparison, the exothermic curves (with cooling rates of 10 and 30°C/min, respectively) for the partially and completely melting samples are presented in Figure 2. As usually expected, the onset crystallization temperatures of the partially melting samples increased distinctly, relative to that of the isotropic melt. For the two cooling rates investigated, the onset crystallization temperatures of the partially melting samples appear ~20°C ahead of those of the completely melting samples. Furthermore, the peak widths are broadened for the two investigated cooling rates. As a matter of fact, for the exothermic curves at other cooling rates, the improvement of the onset crystallization temperatures and broadened peak widths was observed as well. The end-morphologies after nonisothermal crystallization (with cooling rate of 10°C/min) of the partially and completely melting materials are shown in Figure 3. The morphologies indicates that the sizes of the spherulites crystallized from the isotropic melt are not uniform, ranging from 20 to 70 μm [Fig. 3(a)], while for the partially melting materials, the sizes of the spherulites become smaller and uniform, with size of ~30 μm [Fig. 3(b)].

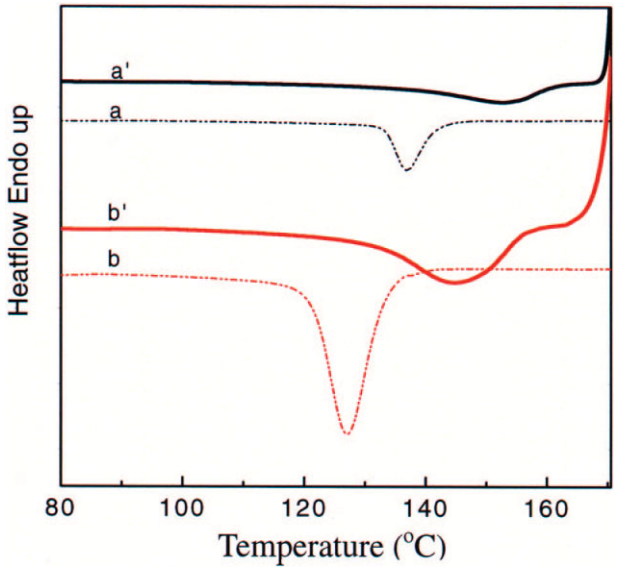

Figure 2 Exothermic curves for partially and completely melting samples.a, cooling at 10°C/min from 200 to 70°C; a′, first crystallized at 145°C for 60 min and then heated to 171°C at 10°C/min, followed by cooling at 10°C/min to 70°C; b, cooling at 30°C/min from 200°C to 70°C; b′, first crystallized at 145°C for 60 min and then heated to 171°C at 10°C/min, and at last followed by cooling at 30°C/min to 70°C. [Color figure can be viewed in the online issue, which is available at www.interscience.wiley.com.].

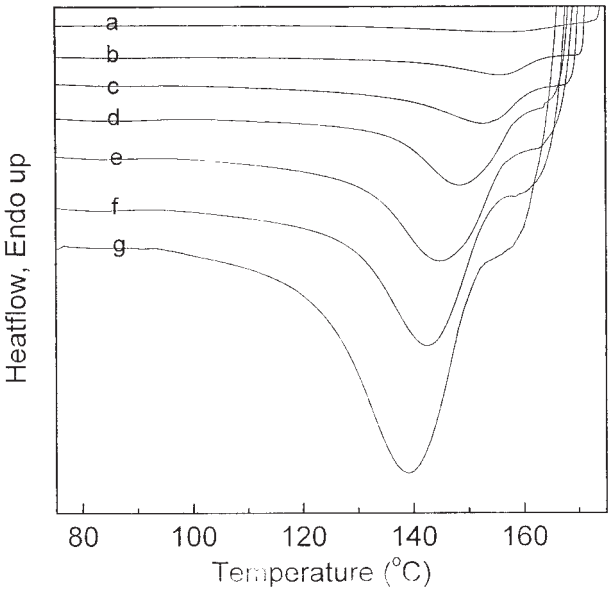

Figure 4 Nonisothermal crystallization exotherm of syndiotactic 1,2-polybutadiene first crystallized at 145°C for 60 min and then heated to 171°C at 10°C/min, and sat last followed by cooling to 70°C at different cooling rates: a, 2.5°C/min; b, 5°C/min; c, 10°C/min; d, 20°C/min; e, 30°C/min; f, 40°C/min; and g, 60°C/min.

The nonisothermal crystallization exotherms of partially melting sPB scanned at seven different cooling rates, ranging from 2.5 to 60°C/min, are indicated in Figure 4. Obviously, the crystallization exotherm becomes wider and shifts to a lower temperature with increasing cooling rate, as was usually observed.

In the nonisothermal crystallization study using DSC instrument, the energy released during the crystallization process appears to be a function of temperature rather than time, as in the case of isothermal crystallization. In this way, the relative crystallinity function of temperature $X_t(T)$ can be formulated as

$$X_t(T) = \frac{\int_{T_0}^{r} \left(\frac{dH_c}{dT}\right) dT}{\Delta H_c} \quad (1)$$

where T_0 and T represent the onset and an arbitrary temperature, respectively, dH_c is the enthalpy of crystallization released during an infinitesimal temperature range dT, and ΔH_c is the total enthalpy of crystallization for a specific cooling rate. To obtain the kinetic information, the experimental data such as those shown in Figure 4 needed to be converted to the relative crystallinity function of temperature $X_t(T)$.

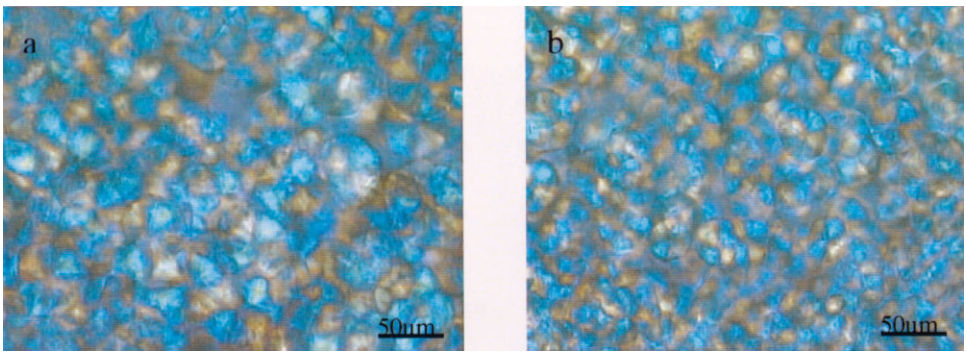

Figure 3 Polarized light microscopy graphs for syndiotactic 1,2-polybutadiene samples crystallized at 145°C for 60 min and heated at 10°C/min from 145 to 200°C (a) and 171°C (b), respectively, and at last followed by cooling to 30°C at 10°C/min. [Color figure can be viewed in the online issue, which is available at www.interscience.wiley.com.].

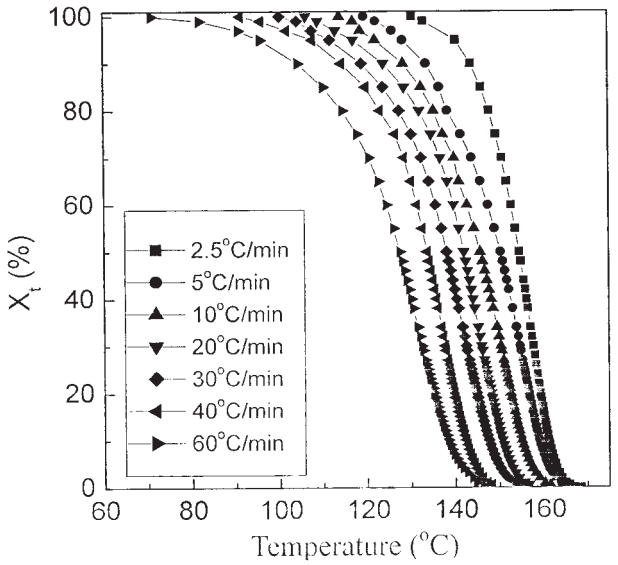

Figure 5 Relative crystallinity of partially melting sPB as a function of temperature at seven different cooling rates. The data were obtained from the exothermic curves using eq. (1).

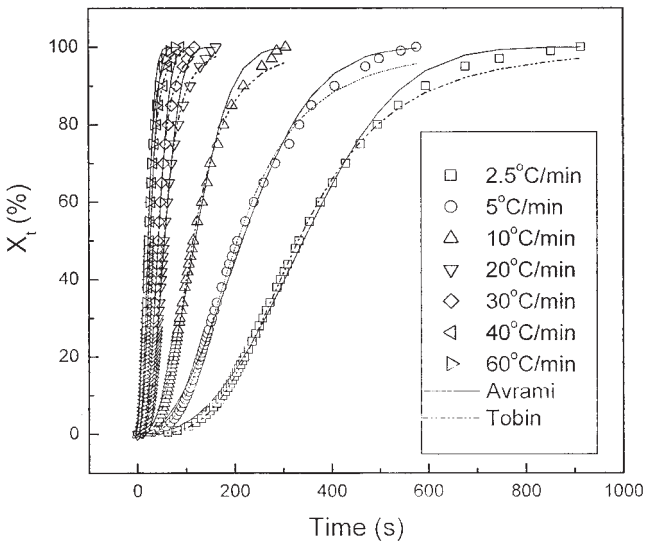

Figure 6 Relative crystallinity of partially melting sPB as a function of time at seven different cooling rates. The data were obtained from Figure 5 using eq. (2). The solid and dotted lines are fitting curves calculated from the Avrami and Tobin Equations, respectively.

The obtained $X_t(T)$ curves are shown in Figure 5. From these curves, some kinetic data such as $T_{0.01}$ (the temperature at 1% relative crystallinity), T_p (the temperature at the maximum crystallization rate or the peak temperature), and $T_{0.99}$ (the temperature at 99% relative crystallinity) are extracted and listed in Table I. Noticeably, the $T_{0.01}$, T_p, and $T_{0.99}$ values are all transferred to lower temperatures when the cooling rate increases. It should be noted that $T_{0.01}$ and $T_{0.99}$ represent the apparent onset and end temperatures of the nonisothermal crystallization process of partially melting materials, respectively.

To analyze nonisothermal crystallization data obtained by DSC using eq. (1), it is assumed that the sample experiences the same thermal history as designated by the DSC furnace. This may be achieved only when the lag between the temperatures of the sample and the furnace is kept minimal. If this assumption is valid, the relation between the crystallization time t and the sample temperature T can be expressed as

TABLE I
Characteristic Data of Nonisothermal Crystallization Exotherms for Self-Seeded Syndiotactic 1.2-Polybutadiene

Φ (°C/min)	$T_{0.01}$ (°C)	T_p (°C)	$T_{0.99}$ (°C)
2.5	165.1	157.5	133
5	163.8	155.3	122.2
10	160.3	150.6	117
20	155.6	144.5	108.9
30	153.4	140.8	104.1
40	147.3	137.0	95.8
60	144.8	131.6	81.9

$$t = \frac{T_0 - T}{\Phi} \tag{2}$$

where Φ is the cooling rate. According to eq. (2), the temperature axis (abscissa) observed in Figure 5 can be transformed into the time scale. The results are exhibited in Figure 6. It is apparent that the faster the cooling rate, the shorter was the time for the completion of the crystallization process. It should be noted that the apparent induction period t_{ind} is very short ($t_{ind} = (T_m - T_{onset})/\Phi$, T_m is the melting point (170.3°C for isothermal crystallization temperature of 145°C), T_{onset} is the actual temperature where the DSC instrument begins to detect the released energy due to crystallization). The t_{ind} values have been calculated and summarized in Table II. The t_{ind} was found to monotonically decrease from ~60 s at 2.5°C/min to ~21.9 s at 60°C/min.

To quantify the kinetics of the nonisothermal crystallization process, the crystallization time at an arbitrary relative crystallinity ($t(X_t)$) can be determined from Figure 6. The $t(X_t)$ values for different relative crystallinities X_t (i.e., 0.01, 0.1, 0.2, 0.4, 0.6, 0.8, 0.9, and 0.99) are summarized in Table II and plotted as a function of cooling rate in Figure 7. The $t_{0.01}$ and $t_{0.99}$ are the qualitative measures of the beginning and the end of the crystallization process. From the values of $t_{0.01}$ and $t_{0.99}$, the apparent total crystallization period Δt_c can be calculated ($\Delta t = t_{0.99} - t_{0.01}$) and the results are summarized in Table II as well. Similarly, the fact that the $t(X_t)$ value for a specific relative crystallinity and the Δt_c value are all found to decrease with in-

TABLE II
The Crystallization Time (t(Xt)) at a Corresponding Relative Crystallinity, the Induction Period (tind), and the Apparent Total Crystallization Period (Dtc), Which were Obtained from Nonisothermal Crystalliztion of Self-Seeded sPB

		$t(X_t)$ (s)								
Φ (°C/min)	t_{ind} (s)	$X_t = 0.01$	$X_t = 0.1$	$X_t = 0.2$	$X_t = 0.4$	$X_t = 0.6$	$X_t = 0.8$	$X_t = 0.09$	$X_t = 0.99$	Δt_c (s)
2.5	60.0	89.9	175	220.3	294.5	385.3	505.4	645.3	860.1	770.2
5	42.0	46.8	101.5	129.4	178	239.6	310.6	406.7	544.2	497.4
10	36.6	27.1	52.9	74	100.2	132.7	170.6	218.9	287.5	260.1
20	32.1	14	26.9	36.5	48.7	61.7	84.7	109.2	154.2	140.2
30	23.2	10.1	18.6	25.1	35	47.5	63.9	80.9	110.6	100.5
40	22.7	7.6	13.1	17.6	25.7	32.6	44.2	62.3	83.1	75.5
60	21.9	5.5	9.1	13.1	19.2	24.8	34.8	45	63.4	57.9

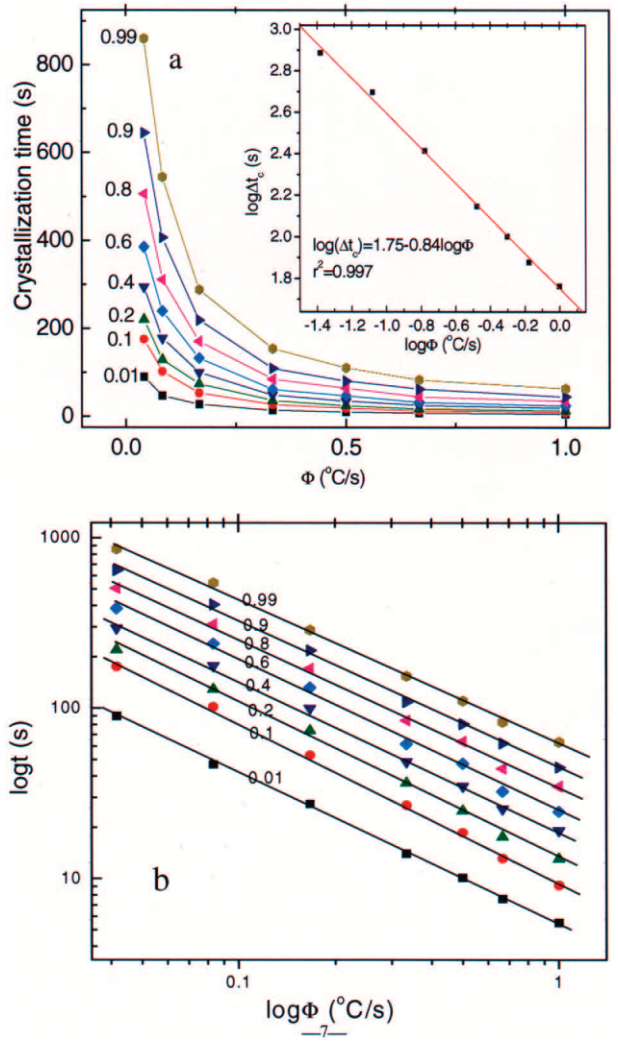

Figure 7 Crystallization time at various relative crystallinity values as a function of cooling rate in linear–linear plot (a) and log–log plot (b), respectively. The inset figure in Fig. 7(a) indicates the relationship between apparent total crystallization period and cooling rate in a log–log plot. [Color figure can be viewed in the online issue, which is available at www.interscience.wiley.com.].

crease in the cooling rate suggests that nonisothermal crystallization proceed faster with increasing the cooling rate. For further analyzing the results obtained, plots of $\log(\Delta t_c)$ vs. $\log \Phi$ [the inserted figure in Fig. 7(a)] and of $\log t(X_t)$ vs. $\log \Phi$ [Fig. 7(b)] are shown. The results indicate that these plots exhibit linear relationship; furthermore, all of the plots exhibit a similar slope (see Table III), with the values -0.89 ± 0.05 $s^2/°C$.

Kinetics analysis of nonisothermal crystallization of partially melting sPB

Avrami analysis

The most common approach to describe the overall isothermal crystallization kinetics is the Avrami model,[28,29] in which the relative crystallinity function of time X_t can be expressed in the following form:

$$X_t = 1 - \exp[-(K_A t)^{n_A}] \varepsilon [0,1] \quad (3)$$

where the parameter K_A is a composite rate constant involving both nucleation and growth rate parameters. The exponent n_A is a constant, which describes the crystallization mechanism and bears relation to

TABLE III
Intercept, Slope, and r^2 Values Obtained by Least Square Method Through Plots of log t_{Xt} versus log Φ for Different Relative Crystallinity Values

Relative crystallinity	Intercept (s)	Slope (s^2/°C)	r^2
0.01	0.74	−0.88	0.999
0.1	0.97	−0.94	0.998
0.2	1.12	−0.91	0.997
0.4	1.28	−0.88	0.997
0.6	1.39	−0.89	0.995
0.8	1.53	−0.87	0.997
0.9	1.65	−0.86	0.998
0.99	1.79	−0.85	0.998
Average		*−0.89*	

TABLE IV
Parameters (n_A, K_A, n_T, K_T) of Crystallization Kinetics for Self-Seeded SPB and the Square of Correlation Coefficients r^2, Obtained by Fitting from Avrami and Tobin Analysis, Respectively, and the Inverse of Crystallization Time at Half Crystallization Degree ($t_{1/2}^{-1}$)

	Avrami analysis			Tobin analysis			
Φ (°C/min)	n_A	K_A ($10^{-3}s^{-1}$)	r^2	n_T	K_T($10^{-3}s^{-1}$)	r^2	$t_{1/2}^{-1}$ (s^{-1})
2.5	2.52	2.53	0.996	3.44	3.02	0.999	321.88
5	2.14	3.91	0.993	3.01	4.86	0.998	195.77
10	2.34	7.21	0.995	3.23	8.75	0.999	107.88
20	2.49	15.25	0.993	3.39	1.82	1	52.64
30	2.67	19.90	0.993	3.64	23.46	1	40.53
40	2.33	31.60	0.993	3.17	38.09	1	25.33
60	2.30	37.71	0.994	3.15	45.66	1	22.16

nucleation type and growth process. It should be noted that the units of K_A are given as an inverse of time. Although the Avrami equation is often used to describe the isothermal crystallization behavior of a semicrystalline polymer, it has also been applied to describe the nonisothermal crystallization behavior of a semicrystalline polymer.[30,31] By fitting the data with different cooling rates in Figure 6 to eq. (3), the Avrami parameters K_A and n_A, together with the r^2 parameters, were obtained from the best fits, the fitting lines (solid line) indicate good fitting. These parameters are listed in Table IV. The Avrami exponent n_A ranged from ~2.1 to 2.7, with the average value being ~2.4 and the standard deviation being ~0.3. The crystallization rate constant K_A is found to increase with the increase of cooling rate, suggesting an improved crystallization rate with increase in cooling rate.

Tobin analysis

In the original derivation of the Avrami model, the effects of growth site impingement and secondary crystallization process were neglected for the purpose of simplicity, which results in the fact that Avrami approach model is only suitable for describing the early stages of crystallization. Tobin proposed a theory for phase transformation kinetics, with consideration of growth site impingement.[32–34] According to this approach, the relative crystallinity function of time X_t can be expressed in the following form:

$$X_t = 1 - \frac{1}{1 + (K_T t)^{n_T}} \varepsilon[0,1] \quad (4)$$

where K_T and n_T are the Tobin crystallization rate constant and the Tobin exponent, respectively. Based on this proposition, n_T need not be an integer[34] and is also governed by different types of nucleation and growth mechanisms. By fitting the data with different cooling rates in Figure 6 to eq. (4) the Tobin kinetic parameters K_T and n_T, together with the r^2 parameters, are obtained from the best fits. The fitting lines are indicated in Figure 6 as dotted lines. These parameters are listed in Table IV. The Tobin exponent n_T was found to range from ~3.0 to 3.60, with the average value being ~3.30 and the standard deviation being ~0.3. The Tobin crystallization rate constant K_T was found to increase with increase in cooling rate, suggesting an increased crystallization rate with increasing cooling rate.

Contrasting the results obtained from avrami and tobin analysis

Comparison of the results in Table IV obtained from the two models indicates that both the Avrami and the Tobin crystallization rate constants (K_A and K_T) are quite comparable, with the K_A value being smaller of the two for a definite cooling rate. The results also indicate that for a given cooling rate, the Avrami exponent n_A is always lower in value than the Tobin exponent n_T. The difference between the values of n_T and n_A is ~0.9, with the standard deviation of ~0.1. For testing the efficiency of the two models, it is better to recalculate the X_t from the parameters listed in Table IV, using eq. (3) and (4) for the Avrami and the Tobin models, respectively. The recalculated X_t curves according to the Avrami and the Tobin models are indicated in Figure 6 as solid and dotted lines. Qualitatively, it is clear that the Tobin model gives a much better prediction of the experimental data than does the Avrami model does.

Ziabicki's kinetic crystallizability analysis

Ziabicki[35–37] suggested that the kinetics of polymeric phase transformation could be described as a first-order kinetic equation.

$$\frac{dX_t}{dt} = K_z(T)(1 - X_t) \quad (5)$$

TABLE V
Parameters Obtained from Ziabicki's Kinetic Crystallizability Analysis on Nonisothermal Crystallization Kinetics for Self-Seeded sPB

Φ (°C/min)	$T_{\max \cdot \Phi}$ (°C)	D_Φ (°C)	$(dX_t/dT)_\Phi$ max	$G_{z,\Phi}$ (°C/min)	G_z
2.5	157.5	13.71	0.53	7.73	3.09
5	155.3	15.73	0.96	16.07	3.21
10	150.6	16.33	1.66	28.84	2.88
20	144.5	16.59	3.63	64.08	3.20
30	140.8	17.28	5.71	104.98	3.50
40	137.0	17.66	6.81	127.96	3.20
60	131.6	19.32	8.49	174.52	2.91

where $K_Z(T)$ is a crystallization rate function with a temperature-dependence. In the case of nonisothermal crystallization, both X_t and $K_Z(T)$ vary and are dependent on the cooling rate.

For a definite cooling rate, the crystallization rate function $K_Z(T)$ can be expressed by a Gaussian function.

$$K_z(T) = K_{z\cdot\max} \exp\left[-\frac{2.773(T - T_{\max})^2}{D^2} \right] \quad (6)$$

where $T_{\max}$ is the temperature at which the crystallization rate is maximum, $K_{Z,\max}$ is the maximum crystallization rate at $T_{\max}$, and D is the width at half-height determined from the crystallization rate function. Using the isokinetic approximation, integration of eq. (6) over the whole crystallizable range (i.e., $T_g < T < T_m^0$) leads to an important characteristic value describing the crystallization ability of a semicrystalline polymer, i.e., the kinetic crystallizability index G_Z:

$$G_z = \int_{T_g}^{T_m^0} K_z(T)dT \approx 1.064 K_{z,\max} D \quad (7)$$

According to the approximate theory,[35] the parameter G_Z describes the ability of a semicrystalline polymer to crystallize when it is cooled at a unit cooling rate.[37]

In the case of nonisothermal crystallization studies using DSC, eq. (7) can be applied when the crystallization rate function $K_Z(T)$ is replaced with a derivative function of the relative crystallinity $(dX/dT)_\Phi$ for each definite cooling rate studied. Therefore, eq. (7) is replaced by

$$G_{z,\Phi} = \int_{T_g}^{T_m^0} \left(\frac{dX_t}{dT} \right)_\Phi dT \approx 1.064 \left(\frac{dX_t}{dT} \right)_{\Phi,\max} D_\Phi \quad (8)$$

where $(dX_t/dT)_{\Phi,\max}$ and D_Φ are the maximum crystallization rate and the width at half-height of the $(dX_t/dT)_\Phi$ function for a definite cooling rate Φ, respectively.

According to eq. (8), $G_{Z,\Phi}$ is the kinetic crystallizability index for an arbitrary cooling rate. The Ziabicki kinetic crystallizability index G_Z can, therefore, be obtained by normalizing $G_{Z,\Phi}$ with Φ

$$G_z = \frac{G_{z,\Phi}}{\Phi} \quad (9)$$

as first suggested by Jeziorny.[38]

According to eq. (8), first differentiate the relative crystallinity function $X_t(T)$ of temperature, as shown in Figure 5, with respect to temperature to obtain the derivative relative crystallinity as a function of temperature $(dX_t/dT)_\Phi$, and then the maximum crystallization rate $(dX_t/dT)_{\Phi,\max}$ and the width D_Φ at the half height can be obtained. Therefore, the cooling-rate-dependent kinetic crystallizability $G_{Z,\Phi}$ can be calculated according to eq. (8) According to eq. (9), the normalized crystallizability index G_Z can be obtained. The temperature at the maximum crystallization rate as determined from the $(dX_t/dT)_\Phi$ function—$T_{\max,\Phi}$, $(dX_t/dT)_{\Phi,\max}$, D_Φ, $G_{Z,\Phi}$, G_Z are calculated and listed in Table V. It should be noteworthy that the $T_{\max,\Phi}$ summarized in Table V and T_p (the peak temperature) in Figure 4 listed in Table I are virtually the same. From Table V, $T_{\max,\Phi}$ was found to decrease, whereas $(dX_t/dT)_{\Phi,\max}$, D_Φ, and $G_{Z,\Phi}$ was found to increase with the increase of cooing rate. After normalizing $G_{Z,\Phi}$ with the cooling rate using eq. (9), the value of the kinetic crystalizability at unit cooling rate G_Z can be determined and the data summarized in Table V indicate that the normalized G_Z values obtained for different cooling rates were almost identical, with the average value being 3.14.

Ozawa analysis

Based on the mathematical derivation of Evans,[39] Ozawa extended the Avrami theory to describe the nonisothermal crystallization case by assuming that the sample was cooled with a constant rate.[40] In the Ozawa method, the time variable in the Avrami equation was replaced by a cooling rate, and the relative

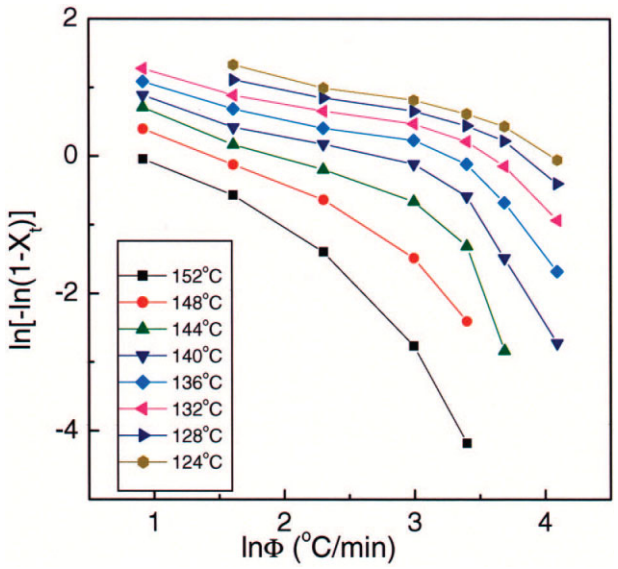

Figure 8 Typical Ozawa plots based on the nonisothermal melt-crystallization data of self-seeded syndiotactic 1,2-polybutadiene. [Color figure can be viewed in the online issue, which is available at www.interscience.wiley.com.].

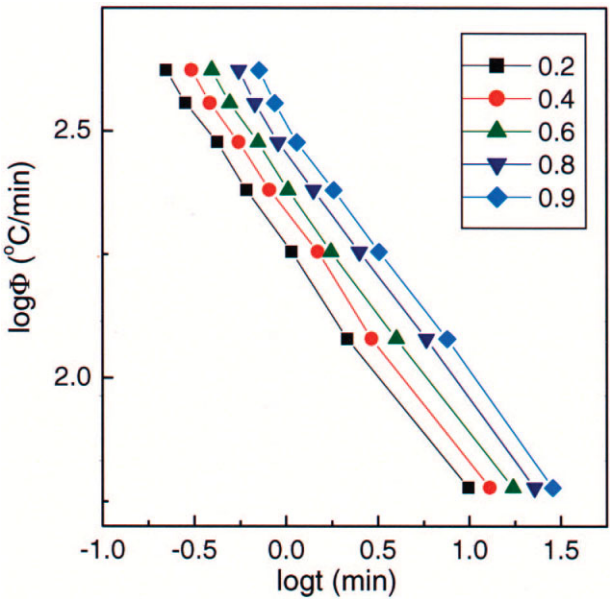

Figure 9 Cooling rates as a function of time at various relative crystallinity based on the combination of the Avrami and Ozawa equations. [Color figure can be viewed in the online issue, which is available at www.interscience.wiley.com.].

crystallinity was derived as a function of constant cooling rate as

$$X_t = 1 - \exp\left[-\left(\frac{K_o}{\Phi}\right)^{n_o} \right] \tag{10}$$

or

$$\ln[-\ln(1 - X_t)] = n_o \ln K_o - n_o \log\Phi \tag{11}$$

where K_O and n_O are the Ozawa crystallization rate constant and the Ozawa exponent, respectively. Both of the Ozawa kinetic parameters (i.e., K_O and n_O) hold similar physical meanings to those of the Avrami ones (i.e., K_A and n_A). The results of the Ozawa analysis are presented in Figure 8 by plotting $\ln[-\ln(1 - X_t)]$ vs. $\ln \Phi$ for specific temperatures ranging from 124 to 152°C. The nonlinear trend in Figure 10 means that the parameter n_O is not a constant during crystallization. As observed for some other polymers,[30,41] the crystallization under nonisothermal condition could not be described by the Ozawa equation. The nonisothermal crystallization of partially melting sPB does not follow the Ozawa equation, probably because of its inaccurate assumption about secondary crystallization.[30]

Combination of avrami and ozawa equations analysis

Mo and coworkers[30,41–43] suggested an equation by combining the Avrami and Ozawa equations, it has successfully described the nonisothermal crystallization process of several samples such as Nylon66, Nylon11, PEDEKK, PAEKEKK, etc as follows:

$$\log\Phi = \log F(T) - a \log t \tag{12}$$

where $a = n_A/n_O$, i.e., the ratio of the Avrami exponent to the Ozawa exponent and the parameter $F(T)$ refers to the value of the cooling rate, which has to be chosen at unit crystallization time when the measured system amounts to a certain degree of crystallinity.

According to eq. (12), the plots of log Φ vs. log t at definite relative crystallinities (0.2, 0.4, 0.6, 0.8, and 0.9) are presented in Figure 9. Good linear relationships between log Φ and log t are obtained. The a, $F(T)$, and r^2 correlation coefficients are obtained by least square method and listed in Table VI. It is clear that a is almost constant, being 1.9, and $F(T)$ increases with increase in crystallinity, suggesting that the higher the

TABLE VI
Parameter Log $F(T)$, a and Correlation Coefficients r^2 Obtained from Mo's Method[30,41–43]

Relative crystallinity	a	log $F(T)$	r^2
0.2	1.9	4.42	0.998
0.4	1.9	4.52	0.998
0.6	2	4.62	0.998
0.8	1.9	4.82	0.998
0.9	1.9	4.92	0.998

relative crystallinity, the higher is the cooling rate needed.

Effective activation energy for nonisothermal crystallization of partially melting sPB

The Avrami, Tobin, Ziabick, Ozawa analysis do not propose a technique for estimating the effective energy barrier for nonisothermal crystallization process ΔE. Kissinger[44] has suggested an expression for evaluating the effective activation energy ΔE, which have correlated the scanning rate Φ with the peak temperature T_p obtained for a given condensed phase transformation. A major problem raised about the use of the expression has been that the original mathematical expression does not permit substitution of negative heating rates (or cooling rates),[45–47] although some works have mistakenly avoided the problem by taking off the minus sign in negative heating rates.[13,24,30,31,41–43] For a process that occurs on cooling, such as nonisothermal crystallization of polymers, reliable value of effective activation energy can be obtained from the integral isoconversional method proposed by Vyazovkin[47] and the differential isoconversional method proposed by Friedman.[48] Because of the simplicity and reliability of Friedman's method, it will be used in this work. The Friedman equation is expressed as[48]:

$$\ln\left(\frac{dX_t}{dt}\right)_{x_t} = A - \frac{\Delta E_{x_1}}{RT} \tag{13}$$

where $(dX_t/dt)_{x_t}$ is the instantaneous crystallization rate function of time at a given relative crystallinity X_t, A is an arbitrary pre-exponential parameter, and ΔE_{x_t} is the effective energy barrier of the process for a given relative crystallinity X_t. By plotting $\ln(dX_t/dt)_{x_t}$ at different cooling rates versus the corresponding reciprocal temperature for a definite X_t, the effective activation energy ΔE_{x_t} for the nonisothermal process can be easily estimated from the slope of the plot by minus slope multiplying R. The ΔE_{x_t} values obtained for different relative crystallinity X_t, ranging from 0.1 to 0.9 with 0.1 increment, are listed in Table VII. Clearly, the ΔE_{x_t} is found to increase monotonically from –170.5 kJ/mol at $X_t = 0.1$ to –86.1 kJ/mol at $X_t = 0.9$.

Evaluation of hoffman-lauritzen parameters (u and k_g) from nonisothermal crystallization

Vyazovkin and Sbirrazzuoli[49] combined Hoffman-Lauritzen theory[50] and isoconversional approach and succeeded in deducing a theoretical formula in which the effective activation energy ΔE is dependent on the temperature as follows:

TABLE VII
Effective Energy Barrier Describing the Overall Nonisothermal Crystallization of Self-Seeded sPB, Obtained from the Differential Isoconversional Method of Friedman

Relative crystallinity	ΔE (kJ/mol)	r^2
0.1	−170.5	0.965
0.2	−165.4	0.976
0.3	−162.6	0.973
0.4	−159.7	0.971
0.5	−158.7	0.962
0.6	−151.5	0.968
0.7	−133.5	0.978
0.8	−101.2	0.972
0.9	−86.1	0.963

$$\Delta E = U\frac{T^2}{(T - T_\infty)^2} + K_g R\frac{T_m^2 - T_m T - T^2}{(T_m - T)^2 T} \tag{14}$$

where U is the activation energy of chain segmental jump, T_m is the equilibrium melting point of this sample (which is 180.9°C for the present sample), T_∞ is a hypothetical temperature at which the motion related to the viscous flow ceases and is usually taken 30 K[50] below the glass transition temperature T_g, and R is the universal gas constant. The kinetics parameter K_g is expressed as:

$$K_g = \frac{n b_0 \delta \delta_e T_m}{k \Delta h_f^n} \tag{15}$$

b_0 is the thickness of a monomolecular layer, δ and δ_e are the lateral and end surface free energies, respectively, k is the Boltzmann constant, Δh_f is the equilibrium melting enthalpy, and n takes 4 for crystallization regime I or III and 2 for crystallization regime II. Using eq.14, Hoffman-Lauritzen parameters U and K_g can be easily evaluated from the nonisothermal crystallization data, using curve fitting of graphics software origin 6.0.[49]

Figure 10(a) presents the dependence of the effective activation energy on the conversation extent. The shape of the curve is similar to that of PET,[49] except the difference of the conversional extent at which inflection occurs. The dependence of the average temperature on the conversion degree is also shown in Figure 10(a). The correlation of the resulting temperature with the conversion extent X_t makes it possible to connect the effective activation energy ΔE to the temperature, according to eq. (14). The variation of the effective activation energy with temperature is shown in Figure 10(b). Vyazovkin and Sbirrazzuoli's[49] predicated that in the temperature region of $0.618T_m - T_m$, ΔE calculated from eq. (14) is negative, and the present data are the cases. Figure 10(b) indicates that the absolute value of the effective activation energy

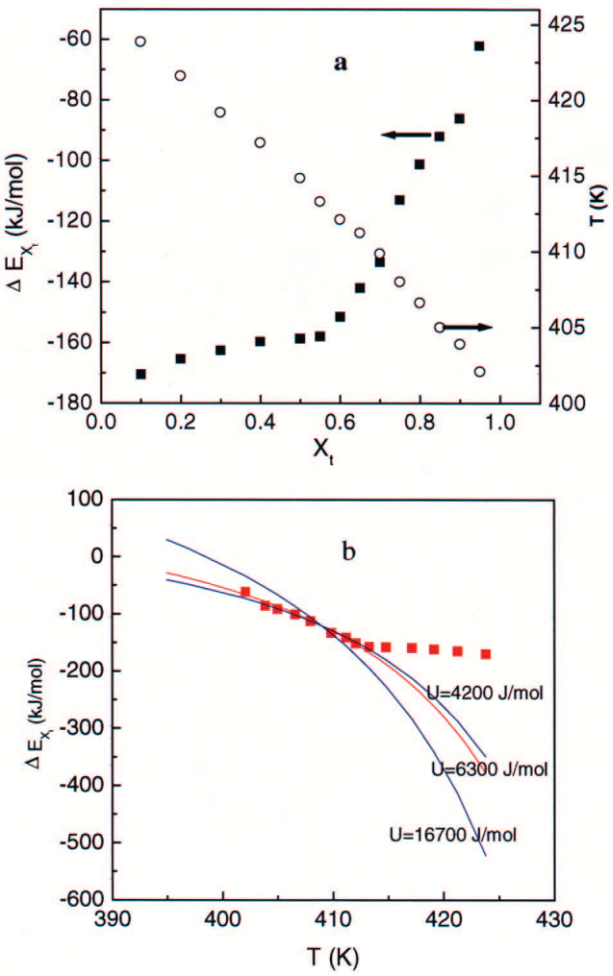

Figure 10 (a) Variation of the effective activation energy with the relative extent of conversion (■) and the variation of the average temperature with the relative extent of conversion (○). (b) Dependence of the effective activation energy on average temperature. The solid lines represent fitting lines for different U values according to eq.14. [Color figure can be viewed in the online issue, which is available at www.interscience.wiley.com.].

ΔE between 424 and 415 K increases slightly with temperature. The nonlinear curve fitting of the data in the temperature range to eq. (14) just obtained a negative U and a smaller positive K_g. Usually U was fixed as 6300 J/mol to fit K_g, if doing so, only one point of the fitting curve intersects with the experiment curve. We considered that the deviant data were derived from the fact that our nonisothermal crystallization experiments were different from those of Vyazovkin and Sbirrazzuoliet et al.'s,[49] the present experiments were carried out under the existence of the remaining crystal nuclei, which reduces the temperature dependence of the nucleation activation energy, thus the total effective activation energy. The other reasons are still kept open to discussion. At higher temperatures corresponding to small undercoolings, possibly, a majority of crystals grow based on the residual crystal nuclei on cooling, thus effective activation energy in temperature range approaching T_m indicates weaker dependence on temperature than that from the pure melt.[49] However, as the temperature is decreased below 415 K, it was found that the effective activation energy ΔE increases with temperature in a steeper trend than in the temperature range above 415 K. We tried to fit the data below 415 K to eq. (14), interestingly finding that Hoffman-Lauritzen parameters U = 6300 J/mol and $K_g = 1.2 \times 10^5$ K^2 can well fit the data. Hoffman et al.[50] have found that the best fit value of U tends to vary between 4200 and 16,700 J/mol, and increasing the value of U results in a larger value of K_g. We fixed the value of U and fit the data below 415 K to eq. (14) and found that K_g increases with increase in the U value, ranging from $K_g = 1.1 \times 10^5$ K^2 for U = 4200 J/mol to $K_g = 1.8 \times 10^5$ K^2 for U = 16,700 J/mol. Figure 10(b) presents the fitting curves for U = 4200, 6300, and 16,700 J/mol. In addition, if not setting the U value during fitting, the last fitted Hoffman-Lauritzen parameters U and K_g are 5200 J/mol and 1.1×10^5 K^2, respectively.

We have also measured the spherulite growth rates of sPB at different temperatures (142, 144, 146, 148, and 150°C) using polarized optical microscopy (POM), according to the well-known Hoffman-Lauritzen theory[50]:

$$G = G_0 \exp\left[-\frac{U}{R(T_c - T_\infty)}\right]\exp\left[-\frac{K_g}{T(T_m - T)f}\right] \quad (16)$$

or

$$\ln G + \frac{U}{R(T_c - T_\infty)} = \ln G_0 \frac{K_g}{T(T_m - T)f} \quad (17)$$

where G is the spherulite growth rate, G_0 is a preexponential factor, and the other parameters have the same physical meanings as indicated in eq. (14). According to eq. (17), by drawing the plot of $\ln G + U/2.3R(T_c - T_\infty)$ versus $1/T_c(T_m - T)f$, as shown in Figure 11, K_g could be easily obtained from minus slope, K_g being 1.3×10^5 K^2. Good agreement was observed on comparing the K_g ($K_g = 1.2 \times 10^5$K^2 for U = 6300 J/mol) obtained by the present DSC method with that ($K_g = 1.3 \times 10^5$ K^2) obtained from POM method.

For clarifying which regime the crystallization data in the investigated temperature region belong to, a Lauritzen test[51] is usually taken on. Z is defined as

$$Z \approx 10^3 (L/2a_0)^2 \exp\left[-\frac{Y}{T_c \Delta T}\right] \quad (18)$$

where L is the effective lamellar thickness and a_0 is the width of molecular chain in crystal. Regime I kinetics

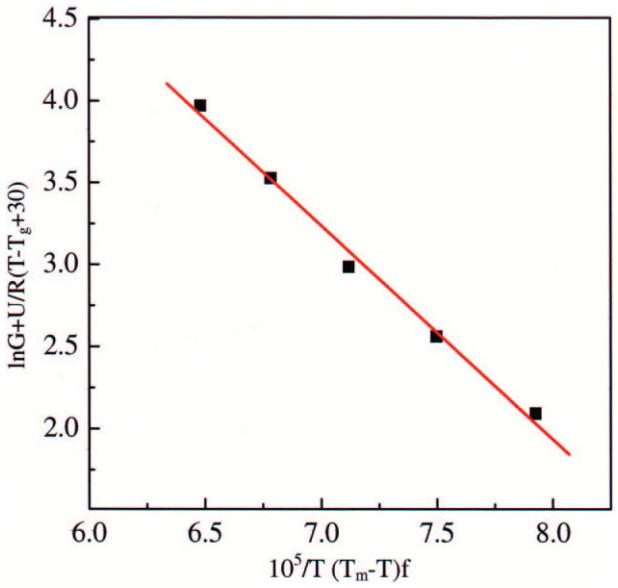

Figure 11 Hoffman-Lauritzen plot for determining nucleation rate constant. [Color figure can be viewed in the online issue, which is available at www.interscience.wiley.com.].

are followed if substitution of $Y = K_g$ into eq. (18) yields $Z \leq 0.01$. If with $Y = 2K_g$, eq. (18) yields $Z \geq 1$, then regime II kinetics are followed, using the dictates of Bavais-Friedel law, which states that the preferred face will be the crystal plane with the largest spacing. Therefore, according to the lattice parameters of sPB, with orthorhombic packaging $a = 1.098$ nm, $b = 0.660$ nm, and $c = 0.514$ nm, proposed by Natta and Corradini,[19] the preferred growth plane will be (110) one, which will give a growth step (i.e., the thickness of a monomolecular layer) $b_0 = 0.641$ nm and the width of the molecular chain $a_0 = 0.566$ nm. With all the aforementioned results, the regime of crystallization is easily determined to be regime II, i.e., numerous surface nuclei involved in formation of substrate, herewith,

$$K_g = 2b_0\delta\delta_e T_m^0/k\Delta h_f^0 \tag{19}$$

From eq. (19), we can calculate the $\delta\delta_e$ product and the work of chain folding q. For obtaining chain folding work q of sPB, lateral surface energy δ must be obtained first. Thomas and stavely[50] developed an approach to evaluate δ as follows:

$$\delta = \alpha\Delta h_f^0 (a_0 b_0)^{\frac{1}{2}} \tag{20}$$

where α is an empirical constant, which usually ranges between 0.1 and 0.3. Commonly, $\alpha = 0.1$ for hydrocarbons such as polyolefins; $\alpha = 0.24$ for polyesters; $\alpha = 0.30$ for most of all organics. Since sPB is attributed to hydrocarbons, furthermore the values of δ and δ_e obtained using $\alpha = 0.24$ and 0.30 are very close, different from the actual crystallization cases of polymers that the surface free energy of the nucleus (δ) is considerably less than the end free energy of the fold surface δ_e. Values of $\alpha = 0.1$will be used. Accordingly, δ was evaluated to be 3.5 erg/cm^2, assnd from the $\delta\delta_e$ product, δ_e was calculated to be 57.9 erg/cm^2.

The work of chain folding, q, per molecular fold can be obtained as[52]

$$\delta_e = \delta_{e0} + \frac{q}{2a_0b_0} \approx \delta + \frac{q}{2a_0b_0} \tag{21}$$

where δ_{eo} is the value that δ_e would assume if no folding work is required. q is the work required to bend a polymer chain back upon itself, considering the conformational constraints on the fold imposed by the crystal structure. As a first approximation, δ_{eo} is approximately equal to the lateral surface energy δ. And as a second approximation, δ_{eo} or δ is much less than $q/2a_0b_0$ and may be regarded as zero. Therefore, eq. (21) is written as

$$q = 2a_0b_0\delta_e \tag{22}$$

It can be seen that for any single polymer chain, δ_e is considered to be inversely proportional to the chain area, the proportion constant being $q/2$. Accordingly, the value of chain folding work is 4.20×10^{-20} J per molecular chain fold, that is, 6.0 kcal/mol.

CONCLUSIONS

The triple melting endothermic peaks were observed for the sPB isothermally crystallized at temperatures ranging from 141 to 149°C, followed by cooling to 70°C. The crystalline materials isothermally crystallized at 145°C were selected for the study of nonisothermal crystallization of partially melting samples. The selected partially melting temperature was 171°C. The onset crystallization temperature for the partially melting materials was improved distinctly relative to that for the isotropic melt. The sizes of the spherulites for the "self-seeded" sPB crystallization are smaller and more uniform than those crystallized from the isotropic melt. The nonisothermal crystallization exotherms of partially melting sPB showed that the temperature at 0.01 relative crystallinity, the peak temperature, and the temperature at 0.99 relative crystallinity all transferred to lower temperatures with increase in cooling rate, indicating that partially melting materials would take shorter time to crystallize as the cooling rate increased. Further data analysis indicated that the apparent induction period, the crystallization time at different relative crystallinity, and the apparent total crystallization period decreased with increasing cooling rate. Both the crystallization time at different relative crystallinity values and the apparent total crys-

tallization period indicated a linear relationship with the cooling rate in the log–log plots, with an average slope of -0.89 $s^2/°C$.

The Avrami and the Tobin models are used to analyze the data and found to describe the nonisothermal crystallization of partially melting sPB very well, with the Tobin model being the better of the two. The average values of the Avrami and Tobin exponents are ~2.4 and 3.3, respectively. Both the Avrami and Tobin crystallization rate constants were found to increase with the increase of cooling rate. The ability of partially melting sPB to crystallize from the self-seeded sPB at a unit cooling rate was estimated based on the Ziabicki's kinetic crystallizability, being 3.14. The Ozawa model could not well describe the nonisothermal crystallization process of partially melting sPB, while the combination of Avrami and Ozawa equations was found to well describe the nonisothermal crystallization of partially melting sPB, with exponent a being 1.9 and the parameter $F(T)$ increasing with increase in relative crystallinity. The effective energy barrier was found to increase monotonically with increase in relative crystallinity. The Hoffman-Lautrizen parameters (U and K_g) were evaluated from data of the nonisothermal crystallization by combining the Hoffman-Lauritzen theory and isoconversional approach. The K_g obtained from DSC technique was found to be in good agreement with that obtained from POM technique.

References

1. Wunderlich, B. Macromolecular Physics; Academic Press: New York, 1976; Vol. 2.
2. Kim, C. Y.; Kim, Y. C.; Kim, S. C. Polym Eng Sci 1991, 31, 1009.
3. Kim, C. Y.; Kim, Y. C.; Kim, S. C. Polym Eng Sci 1993, 33, 1445.
4. Rybnikay, F. J Appl Polym Sci 1982, 27, 1479.
5. Piccarolo, S.; Saiu, M.; Brucato, V.; Titomanlio, G. J Appl Polym Sci 1992, 46, 625.
6. Bank, W.; Gordon, M.; Sharples, A. Polymer 1963, 4, 289.
7. Dai, P. S.; Cebe, P.; Capel, M. J Polym Sci Part B: Polym Phys 2002, 40, 1644.
8. Blundell, D. J.; Keller, A.; Kovacs, A. J. J Polym Sci Polym Lett 1966, 4, 481.
9. Carfagra, C.; Rosa, C. D.; Guerra, G.; Petraccene, V. Polymer 1984, 25, 1462.
10. Fillon, B.; Thierry, A.; Wittmann, J. C.; Lotz, B. J Polym Sci Part B: Polym Phys 1993, 31, 1383.
11. Arnal, M. L.; Muller, A. J. Macromol Chem Phys 1999, 200, 2559.
12. Balsamo, V.; Muller, A. J.; Stadler, R. Macromolecules 1998, 31, 7756.
13. Supaphol, P.; Lin, J. S. Polymer 2001, 42, 9617.
14. Zhu, L.; Calhoun, B. H.; Ge, Q.; Quirk, R. P.; Cheng, S. Z. D.; Thomas, E. L.; Hsiao, B. S.; Yeh, F. J.; Liu, L. Z.; Lotz, B. Macromolecules 2001, 34, 1244.
15. Loo, Y. L.; Register, R. A.; Ryan, A. J. Phys Rev Lett 2000, 84, 4120.
16. Reiter, G. J Polym Sci Part B: Polym Phys 2003, 41, 1869.
17. Pusey, M. L.; Nadarajah, A. Cryst Growth Des 2002, 2, 475.
18. Dubrovskii, V. G. Phys Status Solidi B 1992, 171, 345.
19. Natta, G.; Corradini, P. J Polym Sci 1956, 20, 251.
20. Nir, M. M.; Cohen, R. E. Rubber Chem Tech 1992, 66, 295.
21. Chen, Y.; Yang, D. C.; Hu, Y. M.; Zhang, X. Q. Cryst Growth Des 2004, 4, 117.
22. Tong, C. Y.; Xie, D. M.; Yang, D. C. Chem J Chin Univ 2005, 26, 197.
23. Cai, J. L.; Yu, Q.; Zhang, X. Q.; Lin, J. P.; Jiang, L. S. J Polym Sci Part B: Polym Phys 2005, 43, 2885.
24. Bertini, F.; Canetti, M.; Ricci, G. J Appl Polym Sci 2004, 92, 1680.
25. Sasaki, T.; Sunago, H.; Hoshikawa, T. Polym Eng Sci 2003, 43, 629.
26. Obata, Y.; Homma, C.; Tosaki, C. Polym J 1975, 7, 217.
27. Hu, Y. M.; Dong, W. M.; Jiang, L. S.; Zhang, X. Q. Chin J Catal 2004, 25, 664.
28. Avrami, M. J Chem Phys 1939, 7, 1103.
29. Avrami, M. J Chem Phys 1940, 8, 212.
30. Liu, T. X.; Mo, Z. S.; Zhang, H. F. J Polym Eng 1998, 18, 283.
31. Supaphol, P. J Appl Polym Sci 2000, 78, 338.
32. Tobin, M. C. J Polym Sci Part B: Polym Phys 1974, 12, 399.
33. Tobin, M. C. J Polym Sci Part B: Polym Phys 1976, 14, 2253.
34. Tobin, M. C. J Polym Sci Part B: Polym Phys 1977, 15, 2269.
35. Ziabicki, A. Appl Polym Symp 1967, 6, 1.
36. Ziabicki, A. Polymer 1967, 12, 405.
37. Ziabicki, A. Fundamentals of Fiber Spinning; Wiley: New York, 1976. p 112–114.
38. Jeziorny, A. Polymer 1978, 19, 1142.
39. Evans, U. R. Trans Faraday Soc 1945, 41, 365.
40. Ozawa, T. Polymer 1971, 12, 150.
41. Qiu, Z. B.; Mo, Z. S.; Zhang, H. F.; Sheng, S. R.; Song, C. S. J Macromol Sci Phys 2000, 39, 873.
42. Liu, S. Y.; Yu, Y. Y.; Cui, Y.; Zhang, H. F.; Mo, Z. S. J Appl Polym Sci 1998, 70, 2371.
43. Zhang, Q. X.; Zhang, Z. H.; Zhang, H. F.; Mo, Z. S. J Polym Sci Part B: Polym Phys 2002, 40, 1784.
44. Kissinger, H. Z. J Res Natl Bur Stand 1956, 57, 217.
45. Vyazovkin, S. J Comput Chem 2001, 22, 178.
46. Vyazovkin, S. J Comput Chem 1997, 18, 393.
47. Vyazovkin, S. Macromol Rapid Commun 2002, 23, 771.
48. Friedman, H. J Polym Sci 1965, C6, 183.
49. Vyazovkin, S.; Sbirrazzuoli, N. Macromol Rapid Commun 2004, 25, 733.
50. Hoffman, J. D.; Davis, G. T.; Lauritzen, J. I., Jr. In Treatise on Solid State Chemistry; Hannay, N. B., Ed.; Plenum: New York, 1976; Vol. 3, p 497.
51. Lauritzen, J. I., Jr. J Appl Phys 1973, 44, 4353.
52. Lauritzen, J. I., Jr.; Hoffman, J. D. J Res Natl Bur Stand 1960, 64A, 73.